

# Towards the Evolution of Vertical-Axis Wind Turbines using Supershapes

Richard J. Preen and Larry Bull<sup>1</sup>

**Abstract.** In this paper, we explore the evolution of three-dimensional objects with a simple generative encoding, known as Gielis Superformula. Evolving three-dimensional objects has long been of interest in a wide array of disciplines, from engineering (e.g., robotics) to biology (e.g., studying morphological evolution). While many representations have been presented, ranging from direct encodings to complex graphs and grammars, the vast majority have possessed complex underlying encodings, which were necessary to produce varied morphologies. Here, it is shown possible to produce very closely matching designs of a number of complex three-dimensional objects through the evolution of supershapes produced by Gielis Superformula. Subsequently, we explore the evolution of vertical-axis wind turbine prototypes represented as supershapes wherein each individual is physically instantiated and evaluated under approximated wind tunnel conditions.

## 1 Introduction

In recent years, wind has made an increasing contribution to the world's energy supply mix. However, there is still much to be done in all areas of the technology for it to reach its full potential. Currently, horizontal-axis wind turbines (HAWTs) are the most commonly used form. However, "modern wind farms comprised of HAWTs require significant land resources to separate each wind turbine from the adjacent turbine wakes. This aerodynamic constraint limits the amount of power that can be extracted from a given wind farm footprint. The resulting inefficiency of HAWT farms is currently compensated by using taller wind turbines to access greater wind resources at high altitudes, but this solution comes at the expense of higher engineering costs and greater visual, acoustic, radar and environmental impact" [11]. This has forced wind energy systems away from high energy demand population centres and towards remote locations with higher distribution costs. In contrast, vertical-axis wind turbines (VAWTs) do not need to be oriented to wind direction and can be positioned closely together, potentially resulting in much higher efficiency. VAWT can also be easier to manufacture, may scale more easily, are typically inherently light-weight with little or no noise pollution, and are more able to tolerate extreme weather conditions (see, e.g., [13] for discussions). However, their design space is complex and relatively unexplored. Generally, two classes of design are currently under investigation and exploitation: the Savonius, which has blades attached directly upon the central axis structure; and the Darrieus, where the blades—either straight or curved—are positioned predominantly away from the central structure. Hybrids also exist.

The majority of blade design optimisation is performed through the use of computational fluid dynamics (CFD) simulations, typically described with three-dimensional Navier-Stokes equations [1]. However, three-dimensional CFD simulations are computationally expensive, with a single calculation taking hours on a high-performance computer, making their use with an iterative search approach difficult [18]. Moreover, assumptions need to be made, e.g., regarding turbulence or pressure distributions, which can significantly affect accuracy. Previous evolutionary studies have been undertaken with types of CFD to optimise the blade profile for both HAWT (e.g., [22]) and VAWT (e.g., [8]) to varying degrees of success/realism.

Evolutionary algorithms (EAs) have been used to design three-dimensional physical objects, such as furniture (e.g., [6]), aircraft engine blades (e.g., [35]) and wings (e.g., [46]). Notably, Lohn *et al.* [39] evolved and manufactured X-band satellite antenna for NASA's ST5 spacecraft, representing the world's first artificially evolved hardware in space. Significantly, the antenna's performance was similar to a design hand-produced by an antenna-contractor. Most of these approaches, however, have used simulations to provide the fitness scores of the evolved designs.

The evaluation of physical artifacts for fitness determination can be traced back to the origins of evolutionary computation; for example, the first evolution strategies (ESs) were used to design jet nozzles as a string of real-valued diameters, which were then machined and tested for fitness [52]. Other well-known examples include robot controller design (e.g., [45]), electronic circuit design using programmable hardware (e.g., [59]), product design via human provided fitness values (e.g., [26]), chemical systems (e.g., [58]), and unconventional computers (e.g., [24]). Evolution in hardware has the potential to benefit from access to a richer environment where it can exploit subtle interactions that can be utilised in unexpected ways. For example, the EA used by Thompson [59] to work with field-programmable gate array circuits used some subtle physical properties of the system to solve problems where the properties used are still not understood. Humans can be prevented from designing systems that exploit these subtle and complex physical characteristics through their lack of knowledge, however this does not prevent exploitation through artificial evolution. There is thus a real possibility that evolution in hardware may allow the discovery of new physical effects, which can be harnessed for computation/optimisation [41].

Moreover, the advent of high quality, low-cost, additive rapid fabrication technology—known as three-dimensional printing—means it is now possible to fabricate a wide range of prototype designs quickly and cheaply. Three-dimensional printers are now capable of printing an ever growing array of different materials, including food (e.g., chocolate [23] and meat [38] for culinary design), sugar (e.g., to help create synthetic livers [42]), chemicals (e.g., for custom drug

---

<sup>1</sup> Department of Computer Science and Creative Technologies, University of the West of England, Bristol, BS16 1QY, UK, email: {richard.preen, larry.bull}@uwe.ac.uk

design [57]), cells (e.g., for functional blood vessels [32] and artificial cartilage [62]), plastic (e.g., Southampton University laser sintered aircraft), thermoplastic (e.g., for electronic sensors [36]), titanium (e.g., for prosthetics such as the synthetic mandible developed by the University of Hasselt and transplanted into an 83-year old woman), and liquid metal (e.g., for stretchable electronics [34]). One potential benefit of the technology is the ability to perform fabrication directly in the target environment; for example, Cohen *et al.* [10] recently used a three-dimensional printer to perform a minimally invasive repair of the cartilage and bone of a calf femur *in situ*. Lipson and Pollack [37] were the first to exploit the emerging technology in conjunction with an EA using a simulation of the mechanics and control, ultimately printing mobile robots with embodied neural network controllers.

We have recently undertaken initial experimentation of surrogate-assisted embodied evolutionary algorithms to design VAWT with a vector of integers representing the width of a turbine blade segment [48, 47]. In this paper, we explore the evolution of a simple generative encoding to produce more flexible three-dimensional designs for manufacture by a three-dimensional printer. Initially, the target-based evolution of three-dimensional supershapes is investigated. Subsequently we explore the evolution of VAWT represented as supershapes wherein each individual is physically instantiated and evaluated under approximated wind tunnel conditions.

## 2 Related Work

The evolution of geometric models to design arbitrary three-dimensional morphologies has been widely explored. Early examples include Watabe and Okino's lattice deformation approach [61] and McGuire's sequences of polygonal operators [40]. Sims [55] evolved the morphology and behaviour of virtual creatures that competed in simulated three-dimensional worlds with a directed graph encoding. Bentley [5] investigated the creation of three-dimensional solid objects via the evolution of both fixed and variable length direct encodings. The objects evolved included tables, heatsinks, penta-prisms, boat hulls, aerodynamic cars, as well as hospital department layouts. Eggenberger [12] evolved three-dimensional multicellular organisms with differential gene expression. Jacob and Nazir [31] evolved polyhedral objects with a set of functions to manipulate the designs by adding stellating effects, shrinking, truncating, and indenting polygonal shapes. More recently, Jacob and Hushlak [30] used an interactive evolutionary approach with L-systems [50] to create virtual sculptures and furniture designs.

EAs have also been applied to aircraft wing design (e.g., [46]) including aerodynamic transonic aerofoils (e.g., [20, 51]), and multidisciplinary blade design (e.g., [21]). Few evolved designs, however, have been manufactured into physical objects. Conventionally evolved designs tend to be purely descriptive, specifying what to build but not how it should be built. Thus, there is always an inherent risk of evolving interesting yet unbuildable objects. Moreover, high-fidelity simulations are required to ensure that little difference is observed once the virtual design is physically manifested. In highly complex design domains, such as dynamic objects, the difference between simulation and reality is too large to manufacture designs evolved under a simulator, and in others the simulations are extremely computationally expensive.

Funes and Pollack [15] performed one of the earliest attempts to physically instantiate evolved three-dimensional designs by placing physical LEGO bricks according to the schematics of the evolved individuals. A direct encoding of the physical locations of the bricks

was used and the fitness was scored using a simulator which predicted the stability of the composed structures. Additionally, Hornby and Pollack [28] used L-systems to evolve furniture designs, which were then manufactured by a three-dimensional printer. They found the generative encoding of L-systems produced designs faster and with higher fitness than a non-generative system. Generative systems are known to produce more compact encodings of solutions and thereby greater scalability than direct approaches (e.g., see [54]).

Compositional pattern producing networks [56] have recently been used to evolve three-dimensional objects which were ultimately fabricated on a three-dimensional printer [2, 3, 9]. Both interactive and target-based approaches were explored.

Recently, Rieffel and Sayles [53] evolved circular two-dimensional shapes where each design was fabricated on a three-dimensional printer before assigning fitness values. Interactive evolution was undertaken wherein the fitness for each printed shape was scored subjectively. Each individual's genotype consisted of twenty linear instructions which directed the printer to perform discrete movements and extrude the material. As a consequence of performing the fitness evaluation in the environment, that is, after manufacture, the system as a whole can exhibit epigenetic traits, where phenotypic characteristics arise from the mechanics of assembly. One such example was found when selecting shapes that most closely resembled the letter 'A'. In certain individuals, the cross of the pattern was produced from the print head dragging a thread of material as it moved between different print regions and was not explicitly instructed to do so by the genotype.

Husbands *et al.* [29] used an interactive evolutionary approach to design three-dimensional objects with a superquadrics formula similar to the Gielis Superformula used here. The Genetic Algorithm (GA) [27] used a directed graph encoded as bitstrings that were translated into a valid geometry. They were the first to combine superquadric primitives and global deformations with a GA, incorporating translation, rotation, scaling, reflection, tapering and twisting. A significant advantage of superquadrics is the compactness of the representation since few parameters are needed for a given deformation that widely extends the range of shapes representable.

## 3 Gielis Superformula

Gielis [16, 17] found that the forms of a large variety of plants and other living organisms can be modelled by a single, simple, geometric equation, forming a generalisation of a hyper-ellipse, termed the *Superformula*. Modifying the set of real-valued parameters to the Superformula generates myriad and diverse natural polygons with corresponding degrees of freedom. The Superformula can be used to create three-dimensional objects, *supershapes*, using the spherical product of two superformulas; in fact, by multiplying additional superformulas it can be extended to  $N$ -dimensions. "In general, one could think of the basic Superformula as a transformation to fold or unfold a system of orthogonal coordinate axes like a fan. This creates a basic symmetry and metrics in which distances can further be deformed by local or global transformations. Such additional transformations increase the plasticity of basic Supershapes" [17]. Gielis' Superformula can be further generalised to increase the degrees of freedom, adding twist and further rotations, permitting the creation of more complex three-dimensional forms, including shells, möbius strips, and umbilic tori. Gielis' Superformula, which defines a supershape in 2 dimensions is given in the following equation, where  $r$  is the radius;  $\phi$  is the angle;  $a > 0$ ,  $b > 0$  control the size of the supershape and typically = 1; and  $m$  (symmetry number),  $n_1$ ,  $n_2$  and  $n_3$

(shape coefficients) are the real-valued parameters:

$$r = f(\phi) \frac{1}{\sqrt[n_1]{\left(\left|\frac{1}{a} \cos\left(\frac{m}{4}\phi\right)\right|\right)^{n_2} + \left(\left|\frac{1}{b} \sin\left(\frac{m}{4}\phi\right)\right|\right)^{n_3}}} \quad (1)$$

Using the spherical product, the extension to three dimensions:

$$x = r_1(\theta) \times \cos(\theta) \times r_2(\varphi) \times \cos(\varphi) \quad (2)$$

$$y = r_1(\theta) \times \sin(\theta) \times r_2(\varphi) \times \cos(\varphi) \quad (3)$$

$$z = r_2(\varphi) \times \sin(\varphi) \quad (4)$$

Where  $-\frac{\pi}{2} \leq \varphi \leq \frac{\pi}{2}$  for latitude and  $-\pi \leq \theta \leq \pi$  for longitude.

Example shapes generated with the Superformula can be seen in Figure 1 where the cube, star, and heart can be generated from the same set of eight real-valued parameters; the torus requiring two additional parameters; the shell a total of twelve; and the möbius strip a total of fifteen.

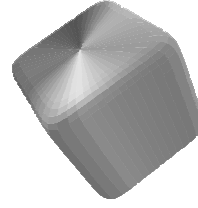
A supershape visualisation tool and its source code, licensed under Creative Commons Attribution-Share Alike 3.0 and GNU GPL license, can be found at <http://openprocessing.org/visuals/?visualID=2638>.

## 4 Target-Based Evolution

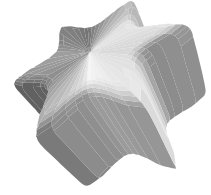
Given a target shape it is often very useful to identify a representative formula. Optimisation methods, such as the Levenberg-Marquardt (LM) theory [49], have typically been used to identify the best fitting supershape parameters (e.g., [19]). However LM cannot retrieve all of the parameters required for supershape fitting. Bokhabrine *et al.* [7] used a GA to evolve all supershape parameters for surface reconstruction (i.e., a target-based approach) using an inside-outside function [14] for fitness computation. Voisin *et al.* [60] later extended this to utilise a pseudo-Euclidean distance for fitness determination, yielding improved performance. Additionally, Morales *et al.* [43] used a GA to evolve  $N$ -dimensional Superformula for clustering.

The cube, star, and heart shapes (as seen in Figure 1) are here converted into  $50 \times 50 \times 50$  binary voxel arrays and used as the desired targets, where the fitness of an individual is the fraction of voxels that correctly match. The genotype of each individual in the population consists of eight real-valued parameters in the range [0,50] which affect the Superformula, giving rise to the supershape. The GA proceeds with a population,  $P$ , of 200 individuals, a per allele mutation rate of 25%, and mutation step size of  $\pm rand(5)$ , where  $rand$  selects a real-valued number in the range [0,5]; a crossover rate of 0%; the GA tournament size for both selection and replacement is set to 3.

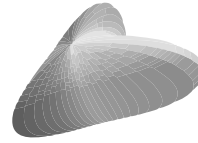
Figures 2–4 show the fraction of total voxels matched to the target shapes during evolution of the supershapes; results presented are an average of 10 experiments. Similar to [9], a large number of voxels are quickly matched, however here the target object is not identifiable until approximately 99% are set correctly. As such, the small differences in fitness between the treatments represent substantial differences in whether the target object is recognisable. In all cases, greater than 99.5% fitness is achieved. From Figure 2 it can be seen that, on average, the GA takes approximately 1100 evaluations to reach >99% matching voxels of a target cube object and 3700 evaluations to achieve >99.9%. Figure 3 shows that on average approximately 3900 evaluations are required to reach >99% matching voxels of a target star object and 16100 evaluations to achieve >99.5%. Finally, Figure 4 shows that, on average, >99% matching voxels of a target heart object is reached after 6400 evaluations and >99.5% after 24000 evaluations.



(a) Cube  $m_1 = 4$ ,  $n_{1,1} = 10$ ,  $n_{1,2} = 10$ ,  $n_{1,3} = 10$ ,  $m_2 = 4$ ,  $n_{2,1} = 10$ ,  $n_{2,2} = 10$ ,  $n_{2,3} = 10$



(b) Star  $m_1 = 6$ ,  $n_{1,1} = 5$ ,  $n_{1,2} = 10$ ,  $n_{1,3} = 10$ ,  $m_2 = 4$ ,  $n_{2,1} = 10$ ,  $n_{2,2} = 10$ ,  $n_{2,3} = 10$



(c) Heart  $m_1 = 3$ ,  $n_{1,1} = 1.5$ ,  $n_{1,2} = 12$ ,  $n_{1,3} = 3$ ,  $m_2 = 0$ ,  $n_{2,1} = 3$ ,  $n_{2,2} = 0$ ,  $n_{2,3} = 0$



(d) Shell  $m_1 = 3$ ,  $n_{1,1} = 1.5$ ,  $n_{1,2} = 12$ ,  $n_{1,3} = 3$ ,  $m_2 = 0$ ,  $n_{2,1} = 3$ ,  $n_{2,2} = 0$ ,  $n_{2,3} = 0$ ,  $t_2 = 2$ ,  $d_1 = 1$ ,  $d_2 = 1$ ,  $c_1 = 5$



(e) Torus  $m_1 = 10$ ,  $n_{1,1} = 10$ ,  $n_{1,2} = 10$ ,  $n_{1,3} = 10$ ,  $m_2 = 10$ ,  $n_{2,1} = 10$ ,  $n_{2,2} = 10$ ,  $n_{2,3} = 10$ ,  $t_1 = 2$ ,  $c_3 = 0$



(f) Möbius Strip  $m_1 = 3$ ,  $n_{1,1} = 1.5$ ,  $n_{1,2} = 12$ ,  $n_{1,3} = 3$ ,  $m_2 = 0$ ,  $n_{2,1} = 3$ ,  $n_{2,2} = 0$ ,  $n_{2,3} = 0$ ,  $t_1 = 4$ ,  $t_2 = 0$ ,  $d_1 = 0$ ,  $d_2 = 0$ ,  $c_1 = 5$ ,  $c_2 = 0.3$ ,  $c_3 = 2.2$

Figure 1: Example three-dimensional supershapes.

At the end of the experiments, the fittest individual was subsequently fabricated by a three-dimensional printer and can be seen in Figure 5, including the supporting rafts required for manufacture. Figure 6 illustrates a sample of the evolved individuals from one cube experiment, Figure 7 similarly for the star experiment, and Figure 8 for the heart experiment.

## 5 Rotation Speed-Based Evolution

As previously mentioned, we have recently undertaken initial experimentation of surrogate-assisted embodied evolutionary algorithms to design VAWT with a vector of integers representing the width of a turbine blade segment [48, 47].

The fitness of each individual was scored as the maximum rotation speed achieved during the application of constant wind generated by an approximated wind tunnel after fabrication by a three-dimensional printer. The rotation speed is the significant measure of aerodynamic efficiency since the design space is constrained (including rotor radius and turbine height). However, in future work, the AC voltage

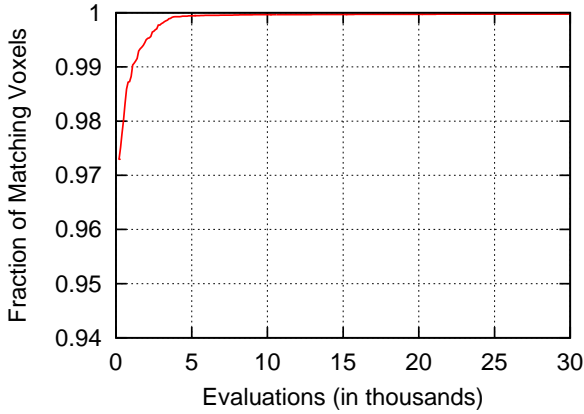


Figure 2: Evolution of a three-dimensional cube.

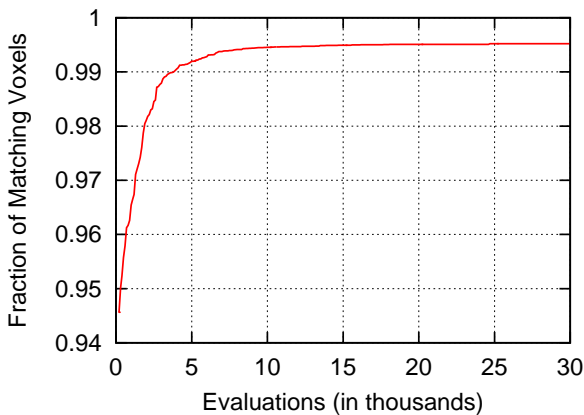


Figure 3: Evolution of a three-dimensional star.

generated would be preferred as it would take into account any slight weight variations that may affect performance. The rotation speed was measured in number of revolutions per minute (*rpm*) using a PCE-DT62 digital photo laser tachometer by placing a  $10 \times 2\text{mm}$  strip of reflecting tape on the outer tip of one of the treatment's blades. When measuring a single isolated VAWT the treatment was placed at  $30\text{mm}$  distance from the centre of a  $3,500\text{rpm}$   $300\text{mm}$  propeller fan generating  $4.4\text{m/s}$  wind speed.

Initially, 20 random designs were generated, fabricated, and evaluated. Since many of the seed treatments were extremely aerodynamically inefficient (only 2 out of 20 yielded  $> 0\text{rpm}$ ), a canonical GA was run for 2 further generations before comparing with a GA assisted by a neural network surrogate model (SGA). The fittest evolved treatments after each generation are reproduced here in Figure 9 for the GA and Figure 10 for the SGA.

Additional challenges are encountered when extracting large amounts of wind energy since multiple turbines must be arranged into a wind farm. As the turbines extract the energy from the wind, the energy content decreases and the amount of turbulence increases downstream from each. See [25] for photographs and explanation of the well-known wake effect at the Horns Rev offshore wind farm in the North Sea. Due to this, HAWTs must be spaced 3–5 turbine diameters apart in the cross-wind direction and 6–10 diameters apart in the downwind direction in order to maintain 90% of the performance of isolated HAWTs [11]. The study of these wake effects is therefore a very complex and important area of research (e.g., see [4]), as is

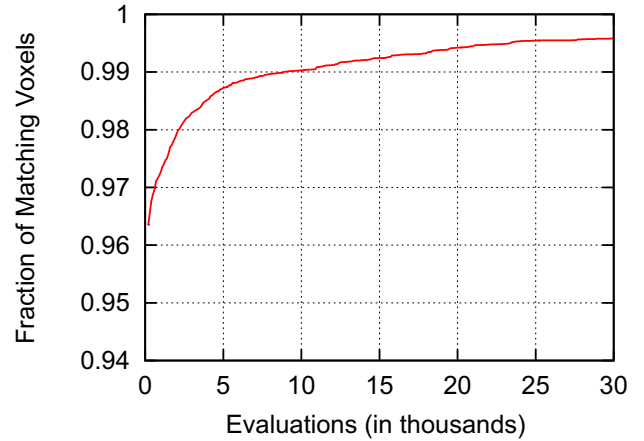


Figure 4: Evolution of a three-dimensional heart.

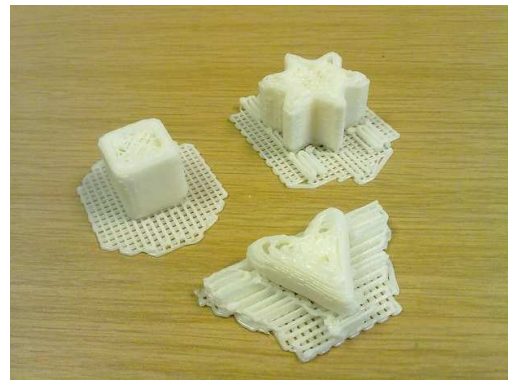


Figure 5: Cube, star and heart fabricated by a three-dimensional printer.

turbine placement (e.g., see [44] for an evolutionary approach). This work has almost exclusively considered HAWT. However, Dabiri *et al.* [33] have recently highlighted how the spacing constraints of HAWT often do not apply for VAWT, and even that performance can be increased by the exploitation of inter-turbine flow effects. Indeed, it has been shown [11] that power densities an order of magnitude greater can be potentially achieved by arranging VAWTs in layouts utilising counter-rotation that enable them to extract energy from adjacent wakes and from above the wind farm.

Therefore, a surrogate-assisted cooperative coevolutionary approach (SCGA) to design wind farms was explored, utilising the aggregated rotation speed of an array of 2 closely positioned VAWT as fitness. Each VAWT was treated separately by evolution and approximation techniques so that heterogeneous designs could potentially emerge. When measuring the fitness of an individual, one turbine from each species population was positioned  $33\text{mm}$  adjacently and  $30\text{mm}$  from the propeller fan. That is, there was a  $3\text{mm}$  spacing between the blades at their closest point. The treatments in each species population were initially evaluated in collaboration with a single randomly selected treatment from the other species population. Thereafter, the GA was run as before, however alternating between species after each offspring was formed and evaluated with the elite member from the other species. The fittest evolved treatments after each generation are shown in Figure 9 for the coevolutionary GA (CGA) and Figure 12 for the SCGA.

The results showed that EAs are capable of identifying novel and increasingly efficient VAWT designs wherein a sample of prototypes

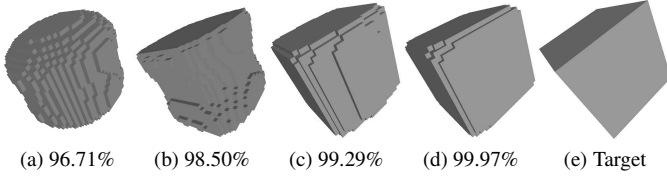


Figure 6: Evolution of a three-dimensional cube.

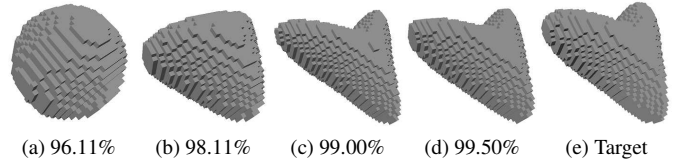


Figure 8: Evolution of a three-dimensional heart.

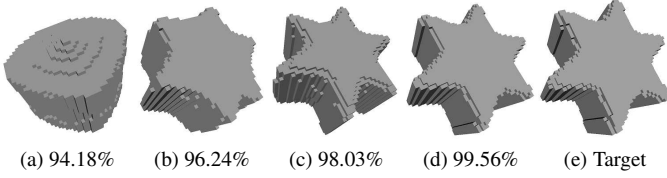


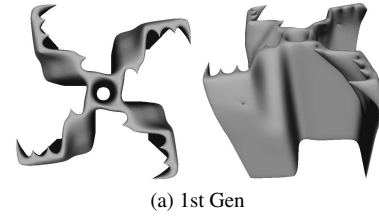
Figure 7: Evolution of a three-dimensional star.

are fabricated by a three-dimensional printer and examined for utility in the real-world. The use of a neural network surrogate model was found to reduce the number of fabrications required by an EA to attain higher aerodynamic efficiency (rotation speed) of VAWT prototypes. The approach represents the first surrogate-assisted embodied evolutionary algorithm using three-dimensional printing, and completely avoids the use of three-dimensional computer simulations, with their associated processing costs and modelling assumptions. In this case, three-dimensional CFD analysis was avoided, but the approach is equally applicable to other real-world optimisation problems, for example, those requiring computational structural dynamics or computational electro-magnetics simulations. In particular, the wind turbine array experiment showed that it is possible to use surrogate-assisted coevolution to iteratively increase the performance of two closely positioned turbines, taking into account the inter-turbine flow effects, which is especially difficult to achieve under a high-fidelity simulation. The surrogate-assisted GA represents a scalable approach to the design of wind turbine arrays since the number of inputs to the surrogate-models remains constant regardless of the number of turbines undergoing evolution.

One of the drawbacks of the representation used is that it assumes an underlying VAWT structure. In contrast, supershapes open the space of possible designs and yet retain a compact encoding. As a first step towards the evolution of supershapes as VAWT, here a single supershape as described previously becomes a prototype VAWT. A workspace (maximum object size) of  $50 \times 50 \times 70mm$  is used so that the instantiated prototype is small enough for timely production ( $\sim 80mins$ ) and with low material cost, yet large enough to be sufficient for fitness evaluation. The workspace has a resolution of  $100 \times 100 \times 100$  voxels. A central platform is constructed for each individual to enable the object to be placed on to the evaluation equipment. The platform consists of a square torus, 2 voxels in width and with a centre of  $10 \times 10$  empty voxels consistent through the  $z$ -axis, thus creating a hollow tube; see example in Figure 13a.

When production is required, the three-dimensional binary voxel array is converted to stereolithography (STL) format. Once encoded in STL, it then undergoes post-processing with the application of 3 Laplacian smoothing steps using Meshlab<sup>2</sup>; see example in Figure 13b. Finally the object is converted to printer-readable G-code

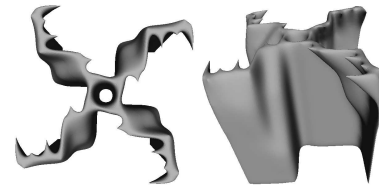
<sup>2</sup> MeshLab is an open source, portable, and extensible system for the processing and editing of unstructured 3D triangular meshes. <http://meshlab.sourceforge.net>



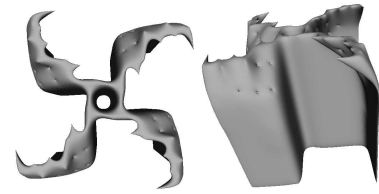
(a) 1st Gen



(b) 2nd Gen



(c) 3rd Gen



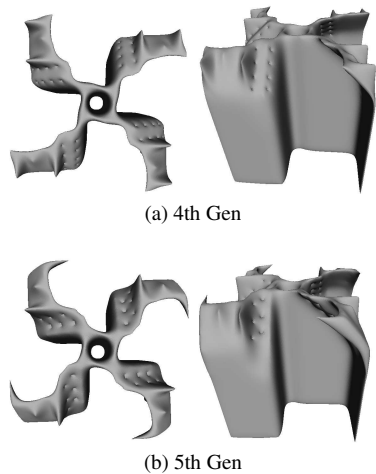
(d) 4th/5th Gen

Figure 9: The fittest treatments with  $z$ -variability produced by the GA each generation.

and is subsequently fabricated by a Stratasys Dimension Elite printer using a polylactic acid (PLA) bioplastic. See example in Figure 13c.

The fitness computation for each individual is the maximum rotation speed achieved during the application of constant wind generated by an approximated wind tunnel after fabrication by a three-dimensional printer. The rotation speed is here measured in number of revolutions per minute ( $rpm$ ) using a PCE-DT62 digital photo laser tachometer by placing a  $10 \times 2mm$  strip of reflecting tape on the centre of the treatment. The experimental configuration can be seen in Figure 14, which shows the 3,  $500rpm$   $300mm$  propeller fan and the treatment placed at  $30mm$  distance and offset by  $100mm$  from the centre; that is, with an asymmetric air flow of  $4.4m/s$ .

The initial population consists of the star individual from Figure 13 and 19 other individuals whose parameters are each those of the star  $\pm rand() \times 5.0$ , where  $rand()$  is a random number in the



**Figure 10:** The fittest treatments with  $z$ -variability produced by the SGA each generation.

range  $[-1,1]$ ; that is,  $P = 20$ . All initial individuals are subsequently fabricated and evaluated. Thereafter, a generational GA forms the next generation using the evolutionary operators as described for the target-based experiment. The fittest evolved treatment after 4 generations is shown in Figure 15. The parameters to the Superformula specify the length of the blades in addition to the frequency and the population has evolved an individual that forms an ‘X’ shape where the blades extend beyond the length of the workspace. As the blades extend beyond the workspace they are no longer drawn/fabricated and so the hollowness of the shape can be observed. It appears that evolution has identified that longer blades are more efficient under the current experimental conditions and this is also observed with an increase in the average length of the blades throughout the population. Furthermore, the reduction in number of blades from the initial 6 to 4 indicates that fewer blades may be more efficient. In Figure 16 the fittest evolved treatment after 5 generations is shown. As can be seen, overall the shape is more rounded and two of the blades from the ‘X’ have merged closer together in a step towards a 3 bladed shape, resulting in a lighter weight design with an increase in rotation speed.

## 6 Conclusions

This paper has shown that it is possible to evolve a vector of reals that are used as Superformula parameters to generate three-dimensional objects. Target-based evolution was used to explore the ability of Superformula to create complex objects, particularly those that resemble natural designs. The experiments showed that with target-based evolution very closely matching objects can be identified. In addition, a methodology for the embodied evolution of supershapes as VAWT has been introduced. One significant advantage of the approach over alternative representations is the simplicity and compactness of the encoding, which may be amenable for use in a surrogate-assisted approach.

If the recent speed and material advances in rapid-prototyping continues, along with the current advancement of evolutionary design, it will soon be feasible to perform a wide-array of automated complex engineering optimisation *in situ*, whether on the micro-scale (e.g., drug design), or the macro-scale (e.g., wind turbine design). That is, instead of using mass manufactured designs, EAs will be used to identify bespoke solutions that are manufactured to compensate and

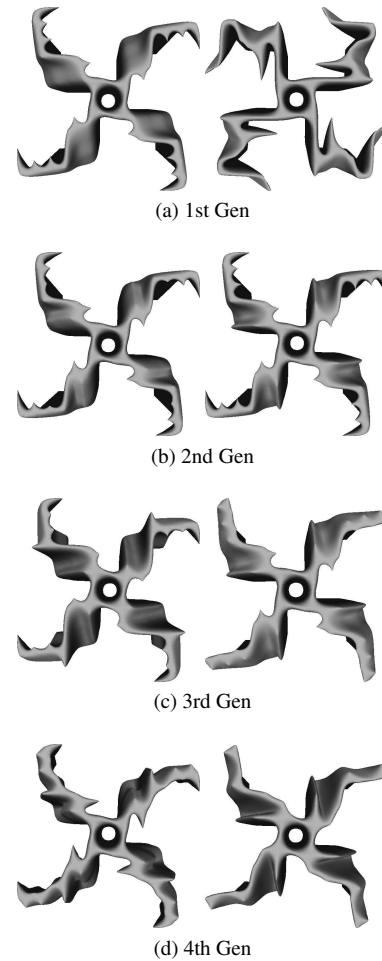


**Figure 11:** Top view of the fittest CGA heterogeneous array treatments each generation. Wind direction from the south.

exploit the specific characteristics of the environment in which they are deployed, e.g., local wind conditions, nearby obstacles, and local acoustic and visual requirements for wind turbines.

## REFERENCES

- [1] John D. Anderson, *Computational Fluid Dynamics: The Basics with Applications*, McGraw Hill, 1995.
- [2] Joshua E. Auerbach and Josh C. Bongard, ‘Dynamic resolution in the co-evolution of morphology and control’, in *12th International Conference on the Synthesis and Simulation of Living Systems*, ALife XII, pp. 451–458. MIT Press, (2010).
- [3] Joshua E. Auerbach and Josh C. Bongard, ‘Evolving CPPNs to grow three-dimensional physical structures’, in *Proceedings of the Genetic and Evolutionary Computation Conference*, pp. 627–634. ACM, (2010).
- [4] R. J. Barthelmie, G. C. Larsen, S. T. Frandsen, L. Folkerts, K. Rados, S. C. Pryor, B. Lange, and G. Schepers, ‘Comparison of wake model simulations with offshore wind turbine wake profiles measured by sodar’, *Atmospheric and Oceanic Technology*, **23**, 888–901, (2006).
- [5] Peter J. Bentley, *Generic Evolutionary Design of Solid Objects using a Genetic Algorithm*, Ph.D. dissertation, University of Huddersfield, 1996.
- [6] Peter J. Bentley and Jonathan P. Wakefield, *Genetic Algorithms in Engineering Systems (GALESIA)*, chapter The Table: An Illustration of Evolutionary Design using Genetic Algorithms, Springer, 1995.
- [7] Y. Bokhabrine, Y. D. Fougere, S. Foufou, and Frédéric Truchetet, ‘Genetic algorithms for Gielis surface recovery from 3D data sets’, in

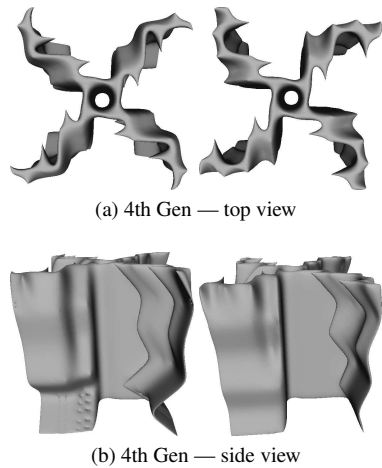


**Figure 12:** The fittest SCGA heterogeneous array treatments. Wind direction from the south.

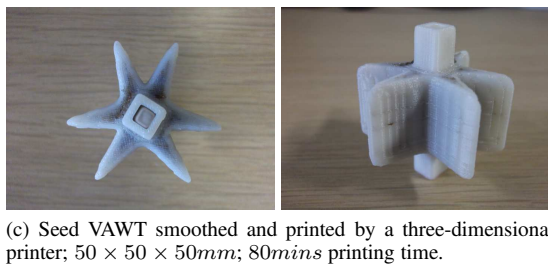
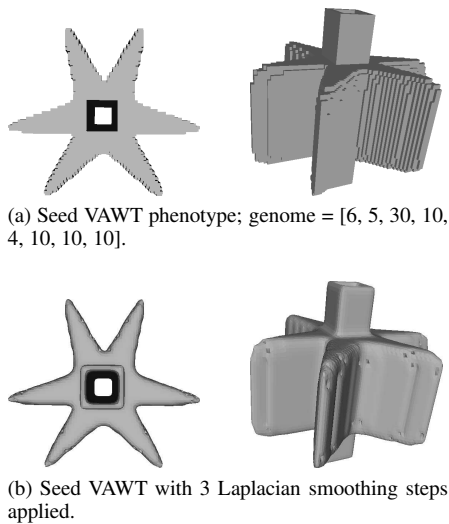


**Figure 13:** Seed VAWT.

- IEEE International Conference on Image Processing*, volume 2 of *ICIP 2007*, pp. 549–552. IEEE Computer Society, (2007).
- [8] Travis J. Carrigan, Brian H. Dennis, Zhen X. Han, and Bo P. Wang, ‘Aerodynamic shape optimization of a vertical-axis wind turbine using differential evolution’, *ISRN Renewable Energy*, (2012).
- [9] Jeff Clune and Hod Lipson, ‘Evolving three-dimensional objects with a generative encoding inspired by developmental biology’, in *Proceedings of the European Conference on Artificial Life*, ECAL ’11, pp. 141–148. MIT Press, (2011).
- [10] Daniel L. Cohen, Jeffrey I. Lipton, Lawrence J. Bonassar, and Hod Lipson, ‘Additive manufacturing for *in situ* repair of osteochondral defects’, *Biofabrication*, **2**(3), (September 2010).
- [11] John O. Dabiri, ‘Potential order-of-magnitude enhancement of wind

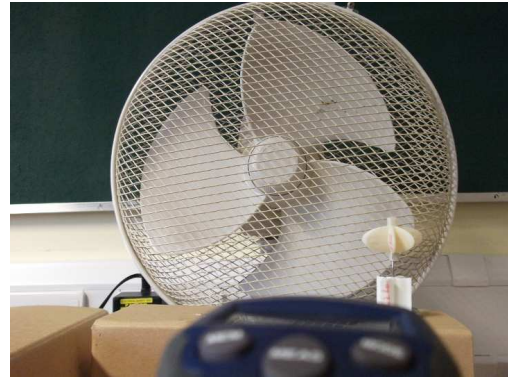


**Figure 14:** VAWT experimental setup.

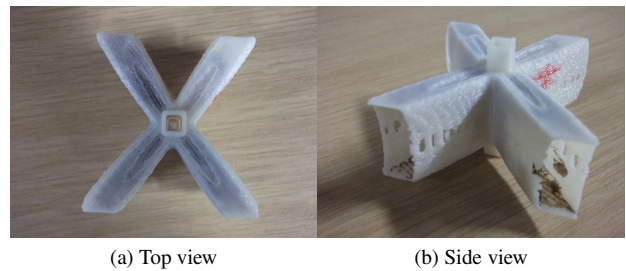


**Figure 15:** Fittest treatment after 4 generations.

- farm power density via counter-rotating vertical-axis wind turbine arrays’, *Journal of Renewable and Sustainable Energy*, **3**(4), (2011).
- [12] Peter Eggenberger, ‘Evolving morphologies of simulated 3D organisms based on differential gene expression’, in *Proceedings of the Fourth European Conference on Artificial Life*, pp. 205–213. MIT Press, (1997).
- [13] S. Eriksson, H. Bernhoff, and M. Leijon, ‘Evaluation of different turbine concepts for wind power’, *Renewable and Sustainable Energy Reviews*, **12**, 1419–1434, (2008).
- [14] Y. D. Fougerolle, A. Gribok, S. Fofou, Frédéric Truchetet, and M. A. Abidi, ‘Supershape recovery from 3D data sets’, in *IEEE International Conference on Image Processing*, ICIP 2006, pp. 2193–2196. IEEE Computer Society, (2006).
- [15] Pablo Funes and Jordan Pollack, ‘Evolutionary body building: Adaptive physical designs for robots’, *Artificial Life*, **4**, 337–357, (October 1998).
- [16] Johan Gielis, ‘A generic geometric transformation that unifies a wide range of natural and abstract shapes’, *American Journal of Botany*, **90**, 333–338, (2003).
- [17] Johan Gielis, Bert Beirinckx, and Edwin Bastiaens, ‘Superquadrics with rational and irrational symmetry’, in *Proceedings of the eighth ACM symposium on Solid modeling and applications*, SM ’03, pp. 262–265. ACM, (2003).
- [18] Lars Gräning, Yaochu Jin, and Bernhard Sendhoff, ‘Individual-based management of meta-models for evolutionary optimization with application to three-dimensional blade optimization’, in *Evolutionary Computation in Dynamic and Uncertain Environments*, eds., Shengxiang Yang, Yew-Soon Ong, and Yaochu Jin, volume 51 of *Studies in Computational Intelligence*, 225–250, Springer, (2007).
- [19] A. Gupta and R. Bajcsy, ‘Volumetric segmentation of range images of 3D objects using superquadrics models’, *Computer Vision, Graphics and Image Processing: Image Understanding*, **58**, 302–326, (1993).
- [20] A. Hacioglu and I. Ozkol, ‘Transonic airfoil design and optimization by using vibrational genetic algorithm’, *Aircraft Engineering and Aerospace Technology*, **75**(4), 350–357, (2003).
- [21] P. Hajela and J. Lee, ‘Genetic algorithms in multidisciplinary rotor blade design’, in *Proc. 36th AIAA/ASME/ASCE/AHS/ASC Structures, Structural Dynamics and Material Conference*, pp. 2187–2197, (1995).
- [22] Mark Hampsey, *Multiobjective Evolutionary Optimisation of Small Wind Turbine Blades*, Ph.D. dissertation, University of Newcastle, 2002.

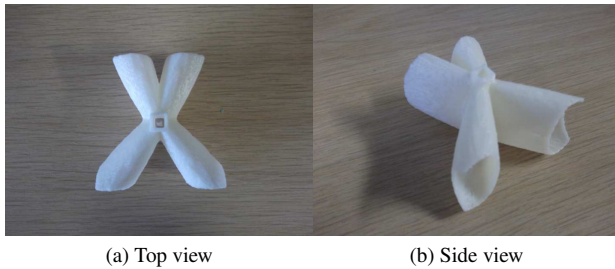


Figure 16: Fittest treatment after 5 generations.

- [23] L. Hao, O. Seaman, S. Mellor, J. Henderson, N. Sewell, and M. Sloan, *Innovative Developments in Design and Manufacturing – Advanced Research in Virtual and Rapid Prototyping*, chapter Extrusion behavior of chocolate for additive layer manufacturing, 245–250, CRC Press, 2009.
- [24] S. L. Harding and J. F. Miller, ‘Evolution in *materio*: Initial experiments with liquid crystal’, in *Proceedings of the NASA/DoD Workshop on Evolvable Hardware*, pp. 289–299. IEEE Computer Society, (2004).
- [25] Charlotte Bay Hasager, Leif Rasmussen, Alfredo Peña, Leo E. Jensen, and Pierre-Elouan Réthoré, ‘Wind farm wake: the Horns Rev photo case’, *Energies*, **6**, 696–716, (2013).
- [26] M. Herdy, ‘Evolution strategies with subjective selection’, in *Parallel Problem Solving from Nature IV*, pp. 22–26. Springer, (1996).
- [27] John Henry Holland, *Adaptation in Natural and Artificial Systems*, University of Michigan Press, 1975.
- [28] Gregory S. Hornby and Jordan B. Pollack, ‘The advantages of generative grammatical encodings for physical design’, in *Proceedings of the IEEE Congress on Evolutionary Computation*, CEC 2001, pp. 600–607. IEEE Computer Society, (2001).
- [29] Phil Husbands, Giles Jermy, Malcolm McIlhagga, and Robert Ives, ‘Two applications of genetic algorithms to component design’, in *Evolutionary Computing*, ed., Terence C. Fogarty, volume 1143 of *Lecture Notes in Computer Science*, 50–61, Springer Berlin Heidelberg, (1996).
- [30] Christian J. Jacob and Gerald Hushlak, ‘Evolutionary and swarm design in science, art, and music’, in *The Art of Artificial Evolution: A Handbook on Evolutionary Art and Music*, 145–166, Springer, (2007).
- [31] Christian J. Jacob and Aamer Nazir, ‘Polyhedron evolver—evolution of 3D shapes with evolvida’, in *Proceedings of the 6th World Multiconference on Systemics, Cybernetics and Informatics: Volume VII Information Systems Development II, July 14–18*. International Institute of Informatics and Systemics, (2002).
- [32] K. Jakab, C. Norotte, B. Damon, F. Marga, A. Neagu, C. L. Besch-Williford, A. Kachurin, K. H. Church, H. Park, V. Mironov, R. Markwald, G. Vunjak-Novakovic, and G. Forgacs, ‘Tissue engineering by self-assembly of cells printed into topologically defined structures’, *Tissue Engineering Part A*, **14**(3), 413–421, (March 2008).
- [33] Matthias Kinzel, Quinn Mulligan, and John O. Dabiri, ‘Energy exchange in an array of vertical-axis wind turbines’, *Journal of Turbulence*, **13**(38), 1–13, (2012).
- [34] C. Ladd, J.-H. So, J. Muth, and M. D. Dickey, ‘3D printing of free standing liquid metal microstructures’, *Advanced Materials*, (doi:10.1002/adma.201301400 2013).
- [35] J. Lee and P. Hajela, ‘Parallel genetic algorithms implementation for multidisciplinary rotor blade design’, *Journal of Aircraft*, **33**(5), 962–969, (1996).
- [36] Simon J. Leigh, Robert J. Bradley, Christopher P. Pursell, Duncan R. Billson, and David A. Hutchins, ‘A simple, low-cost conductive composite material for 3D printing of electronic sensors’, *PLoS ONE*, **7**(11), e49365, (November 2012).
- [37] Hod Lipson and Jordan Pollack, ‘Automatic design and manufacture of robotic lifeforms’, *Nature*, **406**(6799), 974–978, (August 2000).
- [38] J. I. Lipton, D. Arnold, F. Nigl, N. Lopez, D. L. Cohen, Nils Noren, and H. Lipson, ‘Multi-material food printing with complex internal structure suitable for conventional post-processing’, in *21st Solid Freeform Fabrication Symposium*. The University of Texas at Austin, (2010).
- [39] Jason D. Lohn, Gregory S. Hornby, and Derek S Linden, ‘Human-competitive evolved antennas’, *Artificial Intelligence for Engineering Design, Analysis and Manufacturing*, **22**, 235–247, (August 2008).
- [40] Frank McGuire, ‘The origins of sculpture: Evolutionary 3D design’, *IEEE Computer Graphics Applications*, **13**, 9–11, (January 1993).
- [41] J. F. Miller and K. Downing, ‘Evolution in *materio*: Looking beyond the silicon box’, in *Proceedings of the NASA/DoD Workshop on Evolvable Hardware*, pp. 167–176. IEEE Computer Society, (2002).
- [42] Jordan S. Miller, Kelly R. Stevens, Michael T. Yang, Brendon M. Baker, Duc-Huy T. Nguyen, Daniel M. Cohen, Esteban Toro, Alice A. Chen, Peter A. Galie, Xiang Yu, Ritika Chaturvedi, Sangeeta N. Bhatia, and Christopher S. Chen, ‘Rapid casting of patterned vascular networks for perfusable engineered three-dimensional tissues’, *Nature Materials*, **11**, 768–774, (2012).
- [43] Angel Kuri Morales and Edwin Aldana Bobadilla, ‘Clustering with an N-dimensional extension of Gielis Superformula’, in *Proceedings of the 7th WSEAS International Conference on Artificial Intelligence, Knowledge Engineering and Databases*, pp. 343–350. World Scientific and Engineering Academy and Society (WSEAS), (2008).
- [44] G. Mosetti, C. Poloni, and B. Diviacco, ‘Optimization of wind turbine positioning in large wind farms by means of a genetic algorithm’, *Journal of Wind Engineering and Industrial Aerodynamics*, **51**(1), 105–116, (January 1994).
- [45] S. Nolfi, ‘Evolving non-trivial behaviours on real-robots: a garbage collecting robot’, *Robotics and Autonomous Systems*, **22**, 187–198, (1992).
- [46] Y. S. Ong and A. J. Keane, ‘Meta-Lamarckian learning in memetic algorithms’, *IEEE Transactions on Evolutionary Computation*, **8**(3), 99–110, (April 2004).
- [47] Richard J. Preen and Larry Bull, ‘Towards the coevolution of novel vertical-axis wind turbines’, *CoRR*, **abs/1308.3136**, (2013).
- [48] Richard J. Preen and Larry Bull, ‘Towards the evolution of novel vertical-axis wind turbines’, in *Proceedings of the 13th Annual UK Workshop on Computational Intelligence*, UKCI 2013, pp. 74–81. IEEE Computer Society, (2013).
- [49] W. H. Press, S. A. Teukolsky, W. T. Vetterling, and B. P. Flannery, *Numerical Recipes in C: The Art of Scientific Computing (Second Edition)*, Cambridge University Press, 1992.
- [50] Przemysaw W. Prusinkiewicz and Aristid Lindenmayer, *The Algorithmic Beauty of Plants*, Springer, 1990.
- [51] D. Quagliarella and A. D. Cioppa, ‘Genetic algorithms applied to the aerodynamic design of transonic airfoils’, *Journal of Aircraft*, **32**(4), 889–891, (1995).
- [52] Ingo Rechenberg, *Evolutionsstrategie – Optimierung technischer Systeme nach Prinzipien der biologischen Evolution*, Ph.D. dissertation, Technical University of Berlin, 1971.
- [53] John Rieffel and Dave Sayles, ‘EvoFAB: A fully embodied evolutionary fabricator’, in *Evolvable Systems: From Biology to Hardware - 9th International Conference*, eds., Gianluca Tempesti, Andy M. Tyrrell, and Julian F. Miller, ICES 2010, pp. 372–380. Springer, (2010).
- [54] Marc Schoenauer, ‘Shape representations and evolution schemes’, in *Proceedings of the 5th Annual Conference on Evolutionary Programming*, pp. 121–129. MIT Press, (1996).
- [55] Karl Sims, ‘Evolving 3D morphology and behavior by competition’, *Artificial Life*, **1**, 353–372, (1994).
- [56] Kenneth O. Stanley, ‘Compositional pattern producing networks: A novel abstraction of development’, *Genetic Programming and Evolvable Machines*, **8**, 131–162, (2007).
- [57] Mark D. Szymes, Philip J. Kitson, Jun Yan, Craig J. Richmond, Geoffrey J. T. Cooper, Richard W. Bowman, Turfif Vilbrandt, and Leroy Cronin, ‘Integrated 3D-printed reactionware for chemical synthesis and analysis’, *Nature Chemistry*, **4**, 349–354, (2012).
- [58] M. Theis, G. Gazzola, M. Forlin, I. Poli, M. Hanczyc, and M. Bedau, ‘Optimal formulation of complex chemical systems with a genetic algorithm’, *ComplexUs*, (2007).
- [59] A. Thompson, *Hardware Evolution: Automatic design of electronic circuits in reconfigurable hardware by artificial evolution*, Springer, 1998.
- [60] S. Voisin, M. A. Abidi, S. Fofou, and Frédéric Truchetet, ‘Genetic algorithms for 3D reconstruction with supershapes’, in *Proceedings of the IEEE International Conference on Image Processing*, pp. 529–532. IEEE Computer Society, (2009).
- [61] Hirokazu Watabe and Norio Okino, ‘A study on genetic shape design’, in *Proceedings of the 5th International Conference on Genetic Algorithms*, ICGA ’93, pp. 445–451. Morgan Kaufmann Publishers Inc., (1993).
- [62] Tao Xu, Kyle W. Binder, Mohammad Z. Albanna, Dennis Dice, Weixin Zhao, James J. Yoo, and Anthony Atala, ‘Hybrid printing of mechanically and biologically improved constructs for cartilage tissue engineering applications’, *Biofabrication*, **5**(1), (March 2013).